

Peierls Distortion in Two-Dimensional Tight-Binding Model

Yoshiyuki ONO* and Tetsuya HAMANO**

Department of Physics, Toho University, Miyama 2-2-1, Funabashi, Chiba 274-8510

(Received January 26, 2000)

The Peierls distortions in a two-dimensional electron-lattice system described by a Su-Schrieffer-Heeger type model extended to two-dimensions are numerically studied for a square lattice. The electronic band is just half-filled and the nesting vector is $(\pi/a, \pi/a)$ with a the lattice constant. In contrast to the previous understanding on the Peierls transition in two dimensions, the distortions which are determined so as to minimize the total energy of the system involve not only the Fourier component with the nesting wave vector but also many other components with wave vectors parallel to the nesting vector. It is found that such unusual distortions contribute to the formation of gap in the electronic energy spectrum by indirectly (in the sense of second order perturbation) connecting two states having wave vectors differing by the nesting vector from each other. Analyses for different system sizes and for different electron-lattice coupling constants indicate that the existence of such distortions is not a numerical artifact. It is shown that the gap of the electronic energy spectrum is finite everywhere over the Fermi surface.

KEYWORDS: Peierls transition, two-dimensional electron-lattice systems, nesting, Peierls gap, Peierls distortion, second order perturbation

§1. Introduction

The Peierls transition is caused by the freezing of a lattice distortion mode which can connect degenerate electronic states at the Fermi level.¹⁾ The presence of such a distortion induces an energy gap at the Fermi level of the electronic spectrum. This gap which is called Peierls gap lowers the electronic energy. In some cases, this reduction of energy overcomes the increase of the lattice energy due to the frozen mode. In one-dimensional

* E-mail : ono@ph.sci.toho-u.ac.jp

** E-mail : hamano@ph.sci.toho-u.ac.jp

systems, particularly, the lowering of the electronic energy is proportional to the square times logarithm of the frozen mode amplitude and therefore can overcome the lattice energy increase which is proportional to the square of the amplitude. Because of the competition between the decrease of the electronic energy and the increase of the lattice energy, there exists a value of the frozen mode amplitude minimizing the total energy of the electron-lattice system.

In dimensions higher than one, the situation is not so simple. This is because the number of states at the Fermi level is only two in the case of a one-dimensional system, whereas those in two- or three-dimensional systems form equi-energy line or surface, respectively. In general, a single mode of the lattice distortion can connect only two points in the Fermi surface (or line). In this situation, the gain in the electronic energy is too small to overcome the increase of the lattice energy. However, in some special situation where a single lattice distortion mode can connect many states at the Fermi level, the electronic energy is lowered substantially and the Peierls transition becomes possible. This situation is known as “nesting”. The simplest case can be seen in the two-dimensional square lattice tight-binding model with a half-filled electronic band. In this case, the Fermi line is a square within the first Brillouin zone combining four points, $(\pi/a, 0)$, $(0, \pi/a)$, $(-\pi/a, 0)$ and $(0, -\pi/a)$, with a the lattice constant. The nesting vector of this system is $\mathbf{Q} = (\pi/a, \pi/a)$; $\overline{\mathbf{Q}} = (\pi/a, -\pi/a)$ is also a nesting vector, but it is equivalent to \mathbf{Q} .

The Peierls distortion was extensively studied in the late eighties to the early nineties in connection to the high T_c superconductors.^{2,3,4,5)} A typical argument was given, e.g., by Tang and Hirsch³⁾ who used a tight-binding model where the transfer integral is modified by the lattice displacement; its one-dimensional version is known as Su-Schrieffer-Heeger’s (SSH) model.⁶⁾ According to the analysis given in ref. 3, the lattice distortion minimizing the total energy has the wave vector \mathbf{Q} and a polarization parallel to one of the main crystal axes as shown in Fig. 1.

As will be discussed in this paper, the straight forward numerical study of the ground state of the tight-binding square lattice electron-lattice system described by the 2D version of the SSH model indicates that the distortion pattern shown in Fig. 1 does not give the lowest energy state. Fourier analysis of the distortion pattern yielding the lowest energy state shows the freezing of many other modes with wave vectors parallel to \mathbf{Q} in addition to that of the main mode with \mathbf{Q} . We discuss in this paper why this is the case, along with the results of numerical calculations.

In the next section, the model and the method of determining the lowest energy state are described. In § 3, the reason why many modes with wave numbers different from \mathbf{Q} can contribute to lower the total energy will be discussed. Based on the discussion in § 3, we

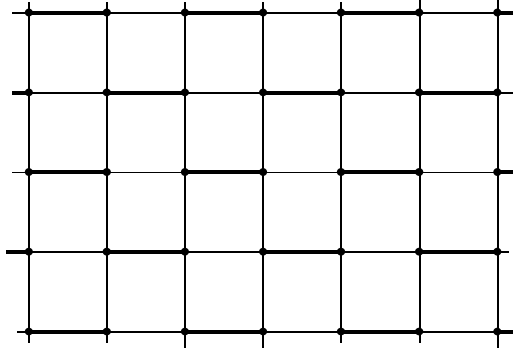


Fig. 1. The asymmetric dimerization pattern. The bonds with thick horizontal lines represent shorter bonds, and the other horizontal bonds are longer ones. There is no dimerization in the perpendicular direction in this situation.

will propose in § 4 a new method to find the lowest energy state, which can reduce a single 2D problem essentially to many 1D problems. The last section is devoted to summary and discussion.

§2. Model and Basic Formulation

The model Hamiltonian treated in this paper is the following SSH-type Hamiltonian extended to two dimensions,

$$\begin{aligned}
 H = & - \sum_{i,j,s} [(t_0 - \alpha x_{i,j})(c_{i+1,j,s}^\dagger c_{i,j,s} + \text{h.c.}) \\
 & + (t_0 - \alpha y_{i,j})(c_{i,j+1,s}^\dagger c_{i,j,s} + \text{h.c.})] \\
 & + \frac{K}{2} \sum_{i,j} (x_{i,j}^2 + y_{i,j}^2), \tag{2.1}
 \end{aligned}$$

where (i, j) represents a lattice point in a square lattice with a lattice constant a , and $x_{i,j} = u_x(i+1, j) - u_x(i, j)$, $y_{i,j} = u_y(i, j+1) - u_y(i, j)$ with $\mathbf{u}(i, j)$ the displacement vector of an ion-unit at the site (i, j) , t_0 the transfer integral of the equidistant (undeformed) lattice, α the electron-lattice coupling constant, $c_{i,j,s}^\dagger$ and $c_{i,j,s}$ the creation and annihilation operators of an electron at the site (i, j) and with spin s . The last term on the right hand side of eq. (2.1) describes the lattice harmonic potential energy with K the force constant. The lattice kinetic energy is omitted since we do not discuss the dynamical problem in this

paper.

If we assume the Peierls distortion having the nesting vector $\mathbf{Q} = (Q_x, Q_y) = (\pi/a, \pi/a)$ as done by Tang and Hirsch,³⁾ the bond variables $x_{i,j}$ and $y_{i,j}$ can be expressed in the following form,

$$x_{i,j} = x_0 e^{i(Q_x i + Q_y j)a} = (-1)^{i+j} x_0, \quad (2.2)$$

$$y_{i,j} = y_0 e^{i(Q_x i + Q_y j)a} = (-1)^{i+j} y_0, \quad (2.3)$$

where x_0 and y_0 are the amplitudes of the distortion to be determined to minimize the total energy of the system. In this situation the electronic part of the above Hamiltonian can be easily diagonalized by introducing the Fourier expansion of the electronic field operators as follows,

$$c_{i,j} = \frac{1}{N} \sum_{\mathbf{k}} c_{\mathbf{k}} e^{i(k_x i + k_y j)a}, \quad (2.4)$$

where N^2 is the total number of lattice points and the components of the wave vector $\mathbf{k} = (k_x, k_y)$ are given by integer times $2\pi/Na$, respectively, on the assumption of the periodic boundary conditions. The diagonalization process is straightforward, and the ground state energy of the system is expressed in the form,

$$E_{\text{tot}}^{\text{GS}} = -2 \sum'_{\mathbf{k}} E_{\mathbf{k}} + N^2 \frac{K}{2} (x_0^2 + y_0^2), \quad (2.5)$$

where the sum over the wave vector \mathbf{k} is restricted to the region satisfying the following two conditions,

$$-\frac{\pi}{a} < k_x + k_y \leq \frac{\pi}{a} \quad (2.6)$$

$$-\frac{\pi}{a} < k_x - k_y \leq \frac{\pi}{a} \quad (2.7)$$

and $E_{\mathbf{k}}$ is given by

$$E_{\mathbf{k}} = \sqrt{\varepsilon_{\mathbf{k}}^2 + \Delta_{\mathbf{k}}^2} \quad (2.8)$$

with $\varepsilon_{\mathbf{k}} = -2t_0(\cos k_x a + \cos k_y a)$ and $\Delta_{\mathbf{k}} = 2\alpha(x_0 \sin k_x a + y_0 \sin k_y a)$. The factor 2 in front of the \mathbf{k} -sum in eq. (2.5) is due to the spin degeneracy. The boundary determined by the conditions eqs. (2.6) and (2.7) is nothing but the Fermi surface (or line since the present system is two dimensional) and on this boundary $\varepsilon_{\mathbf{k}}$ vanishes. Across this boundary the electronic energy band is divided into two pieces, the dispersions of the lower and upper bands being expressed by $-E_{\mathbf{k}}$ and $E_{\mathbf{k}}$, respectively. This means that the energy gap at the Fermi surface is given by $2|\Delta_{\mathbf{k}}|$.

According to Tang and Hirsch,³⁾ the dimerization pattern shown in Fig. 1 which is realized by setting $x_0 \neq 0$ and $y_0 = 0$ or vice versa and therefore highly asymmetric in x and y

directions can have lower energy than the symmetric dimerization realized when $x_0 = y_0 \neq 0$ (or equivalently $x_0 = -y_0$). It is not difficult to understand the reason if we see the expression of $\Delta_{\mathbf{k}}$ for each case; in the asymmetric case, $\Delta_{\mathbf{k}}^{\text{asym}} = 2\alpha x_0 \sin k_x a$, and in the symmetric case, $\Delta_{\mathbf{k}}^{\text{sym}} = 4\alpha x_0 \sin[\frac{1}{2}(k_x + k_y)a] \cos[\frac{1}{2}(k_x - k_y)a]$. The gap on the Fermi surface does not vanish except for the points $(0, \pi/a)$ and $(\pi/a, 0)$ in the case of the asymmetric dimerization. On the other hand the gap vanishes on the line $k_x - k_y = \pi/a$ in the case of symmetric dimerization. We have confirmed numerically that if we fix the ratio $r = y_0/x_0$ ($0 \leq r \leq 1$) and minimize the total energy with respect to x_0 , then the minimum value of the energy is a monotonically increasing function of r and becomes the smallest at $r = 0$.

It is clear that the dimerization pattern shown in Fig. 1 can yield the lowest energy state as far as we consider only the distortion with the basic nesting vector \mathbf{Q} . However, we should note that even in this asymmetric dimerization the gap vanishes at some special points on the Fermi surface. In general the Peierls gap is proportional to the matrix element of the electron-lattice coupling term in H between two electronic states with wave vectors \mathbf{k} and $\mathbf{k} \pm \mathbf{Q}$. In the case of the SSH-type Hamiltonian as used in this paper, this matrix element is given by a linear combination of $\sin k_x a$ and $\sin k_y a$. It vanishes at $(\pi/a, 0)$ and $(0, \pi/a)$ irrespectively of the lattice dimerization pattern. This means that the degeneracy between $(\pi/a, 0)$ and $(0, -\pi/a)$ [or between $(0, \pi/a)$ and $(-\pi/a, 0)$] cannot be removed within the first order perturbation due to the lattice distortion with \mathbf{Q} . We shall come back to this problem in § 4.

§3. Numerical Study

In order to check whether the asymmetric dimerization pattern shown in Fig. 1 can yield the lowest energy state or whether there exist any different dimerization patterns giving still lower energy, we have studied numerically the lowest energy state of the Hamiltonian eq. (2.1). Once we know the local values of $x_{i,j}$'s and $y_{i,j}$'s, the electronic wave functions $\{\phi_\nu(i, j)\}$ are calculated along with corresponding eigenenergies $\{\varepsilon_\nu\}$ from the following Schrödinger equation,

$$\begin{aligned} \varepsilon_\nu \phi_\nu(i, j) = & -(t_0 - \alpha x_{i,j})\phi_\nu(i + 1, j) \\ & -(t_0 - \alpha x_{i-1,j})\phi_\nu(i - 1, j) \\ & -(t_0 - \alpha y_{i,j})\phi_\nu(i, j + 1) \\ & -(t_0 - \alpha y_{i,j-1})\phi_\nu(i, j - 1)]. \end{aligned} \quad (3.1)$$

Since the number of electrons is fixed, it is straightforward to obtain the electronic ground state energy for the given configurations of $x_{i,j}$'s and $y_{i,j}$'s. The bond length variables $x_{i,j}$'s and $y_{i,j}$'s are also involved in the lattice potential energy, and they are determined so as to

minimize the total energy of the system. This condition yields the following self-consistent equations for these variables similarly as in one-dimensional cases,^{7,8)}

$$x_{i,j} = -\frac{2\alpha}{K} \sum_{\nu}' \phi_{\nu}(i+1, j) \phi_{\nu}(i, j) + \frac{2\alpha}{NK} \sum_{i'} \sum_{\nu}' \phi_{\nu}(i'+1, j) \phi_{\nu}(i', j), \quad (3.2)$$

$$y_{i,j} = -\frac{2\alpha}{K} \sum_{\nu}' \phi_{\nu}(i, j+1) \phi_{\nu}(i, j) + \frac{2\alpha}{NK} \sum_{j'} \sum_{\nu}' \phi_{\nu}(i, j'+1) \phi_{\nu}(i, j'), \quad (3.3)$$

where the summation over the one particle states ν is restricted to the occupied ones in the electronic ground state; note that the spin degeneracy factor should be included. The second terms on the right hand sides are due to the periodic boundary conditions, which require $\sum_{i=1}^N x_{i,j} = 0$ for arbitrary j and $\sum_{j=1}^N y_{i,j} = 0$ for arbitrary i .

In most of the practical calculations we use typically the following values of parameters; $t_0 = 2.5\text{eV}$, $K = 21.0\text{eV}/\text{\AA}^2$ and $\alpha = 4.0\text{eV}/\text{\AA}$. These values are near to those for polyacetylene. As is well known what is important in this type of electron-lattice systems is the dimensionless coupling constant defined by $\lambda = \alpha^2/Kt_0$. Aforementioned values of parameters give $\lambda \simeq 0.30$. When we want to study the coupling constant dependence of various properties, only the value of α is changed for simplicity.

The set of self-consistent equations (3.1) to (3.3) can be solved numerically by iteration. First we give initial values for $x_{i,j}$'s and $y_{i,j}$'s, and then calculate $\phi_{\nu}(i, j)$'s by a matrix diagonalization subroutine, the results of which are substituted into the right hand sides of eqs. (3.2) and (3.3). The resulting values of $x_{i,j}$'s and $y_{i,j}$'s are compared with the previous values. If the difference is not small, we proceed by replacing the initial values of $x_{i,j}$'s and $y_{i,j}$'s by new ones. This procedure is continued until the difference becomes negligibly small.

We try three different initial configurations. First one is the asymmetrically dimerized pattern as shown in Fig. 1. If we start the iteration with the uniform dimerization as expressed by eqs. (2.2) and (2.3) by setting $y_0 = 0$ and giving an appropriate value of the order of $10^{-2}a$ for x_0 , we end up with the same pattern with a value of x_0 which minimizes the total energy of the system within that pattern. The second choice is the symmetrically dimerized pattern as given by eqs (2.2) and (2.3) with $x_0 = y_0 \neq 0$. The third one is a random distortion; we give random values for the lattice displacement vectors $\{\mathbf{u}(i, j)\}$ with a relatively small amplitude of the order of $10^{-2} \times a$; many samples are studied in this treatment. The last two choices yield essentially the same result. The resulting distortion pattern is not described by eqs. (2.2) and (2.3). An example of Fourier analysis of this

pattern is shown in Fig. 2, where $X(q_x, q_y)$ and $Y(q_x, q_y)$ are defined by

$$X(q_x, q_y) = \frac{1}{N^2} \sum_{i,j} x_{i,j} \exp[-i(q_x i + q_y j)a], \quad (3.4)$$

$$Y(q_x, q_y) = \frac{1}{N^2} \sum_{i,j} y_{i,j} \exp[-i(q_x i + q_y j)a]. \quad (3.5)$$

We have found that all the Fourier components with $q_x \neq q_y$ vanish.⁹⁾

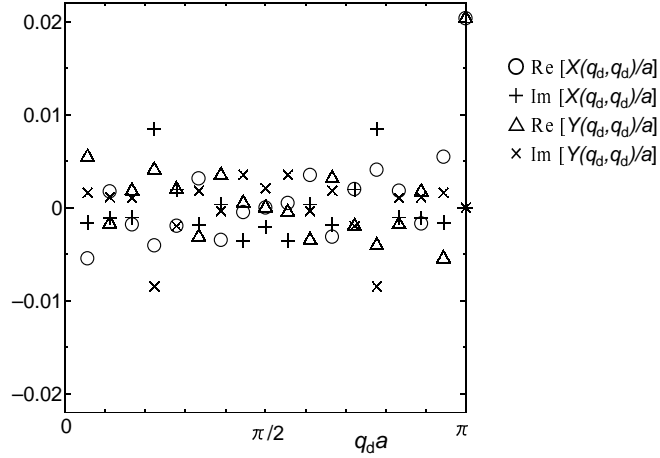


Fig. 2. The Fourier spectra of the distortion pattern obtained by numerical minimization of the total energy. As for the direction of the wave number \mathbf{q} , the Fourier components vanish when $q_x \neq q_y$. The abscissa indicates $q_d a$ ($= q_x a = q_y a$). The system size is 36×36 . The electron-lattice coupling constant α is equal to $4.0\text{eV}/\text{\AA}^2$ which corresponds to $\lambda = 0.30$.

What is characteristic in these Fourier spectra is that the amplitudes [= $\sqrt{|X(\mathbf{q}_i)|^2 + |Y(\mathbf{q}_i)|^2}$ ($i = 1, 2$)] of two modes with \mathbf{q}_1 and \mathbf{q}_2 satisfying the condition $\mathbf{q}_1 + \mathbf{q}_2 = \mathbf{Q}$ are equal to each other. The meaning of this property will be discussed in the next section. It should be noted that as far as the \mathbf{Q} -components are concerned the amplitudes are highly isotropic in x and y directions.

The electronic energy spectrum corresponding to this lattice configuration is different from that in the asymmetric dimerization case (Fig. 1). There is no point on the Fermi surface where the Peierls gap vanishes. The behavior of the gap along the Fermi surface will be discussed later in detail.

In order to check whether this complicated state has a lower energy than the asymmetrically dimerized state as shown in Fig. 1, we study the size dependence of the energy difference between the asymmetrically dimerized state (Fig. 1) and the lowest energy state obtained by solving the self-consistent equations (3.1) to (3.3); the total energy of the former state is denoted by E_A and the latter by E_G , both of them being negative. The result is summarized in Fig. 3, where the energy difference scaled by $|E_A|$ is plotted as a function of N^{-2} , the inverse of the total number of the lattice points, for two different values of α , other parameters being fixed as mentioned before.

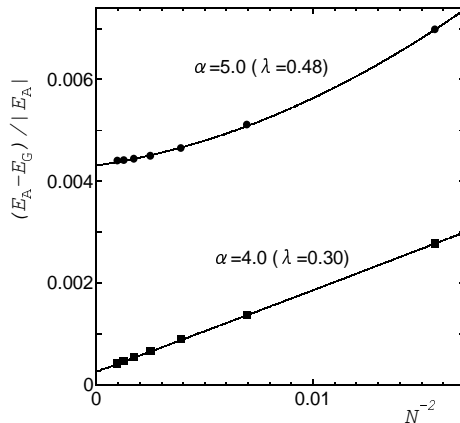


Fig. 3. The size-dependence of the energy difference between the asymmetrically dimerized state and the lowest energy state obtained by solving the self-consistent equations. The abscissa is the inverse of the total number of the lattice points. The value of α is indicated in the figure along with the corresponding value of the dimensionless coupling constant λ , other parameters being fixed ($t_0 = 2.5\text{eV}$ and $K = 21.0\text{eV}/\text{\AA}^2$). The continuous lines are fitting to quadratic polynomials.

From Fig. 3, we may safely conclude that the energy difference remains finite in the thermodynamic limit, and that the lowest energy state obtained from the self-consistent equation has certainly a smaller energy than the asymmetrically dimerized state shown in Fig. 1.

§4. Peierls Gap due to Second Order Process

In this section we discuss why the single mode dimerization (Fig. 1) is not the lowest energy state. The lowest energy state obtained numerically in the previous section involves

multi-mode distortions. The Fourier analysis of the distortions indicates that the gap in the electronic spectrum is induced not only by the first order perturbation but also by the second order process. As discussed in § 1, the Peierls gap in the electronic spectrum is formed usually by the first order process in which a state $|\mathbf{k}\rangle$ on the Fermi surface is coupled to another state $|\mathbf{k} \pm \mathbf{Q}\rangle$ on the Fermi surface by the lattice distortion with a wave vector \mathbf{Q} (the nesting vector). The consideration developed in § 2 indicates that the gap vanishes at special points on the Fermi surface, $(\pi/a, 0)$ and $(0, \pi/a)$, by this first order process because of the peculiar wave number dependence of the electron-lattice coupling term. This fact means that in order to get a finite gap at those point we have to consider the second order process where at least two lattice distortion modes should be relevant.

If two distortion modes with wave vectors \mathbf{q}_1 and \mathbf{q}_2 satisfying $\mathbf{q}_1 + \mathbf{q}_2 = \mathbf{Q}$ are involved in the second order process, there should appear matrix elements connecting one of the states $|\mathbf{k}\rangle$ or $|\mathbf{k} + \mathbf{Q}\rangle$ and one of $|\mathbf{k} + \mathbf{q}_1\rangle$ or $|\mathbf{k} + \mathbf{q}_2\rangle$, where the former states are on the Fermi surface. This indicates in turn that the two states $|\mathbf{k} + \mathbf{q}_1\rangle$ and $|\mathbf{k} + \mathbf{q}_2\rangle$ which are not on the Fermi surface are mixed with the states $|\mathbf{k}\rangle$ and $|\mathbf{k} + \mathbf{Q}\rangle$ on the Fermi surface and contribute to the formation of the gap at the Fermi surface. In such a situation it is natural to expect the creation of lattice distortions with wave vectors $\mathbf{q}_1 - \mathbf{q}_2$, $\mathbf{q}_2 - \mathbf{q}_1$, $\mathbf{q}_1 - \mathbf{q}_2 + \mathbf{Q}(= 2\mathbf{q}_1)$ and $\mathbf{q}_2 - \mathbf{q}_1 + \mathbf{Q}(= 2\mathbf{q}_2)$. In this way, many lattice distortion modes can be involved in the second order process.

Based on the numerical results discussed in the previous section, we assume that, in the lowest energy state, only the lattice distortions with wave vectors parallel to \mathbf{Q} are existing. Namely the bond variables $x_{i,j}$ and $y_{i,j}$ are assumed to be expressed in the form,

$$x_{i,j} = x_0(-1)^{i+j} + \sum_{0 < q < \pi/a} [x_q e^{iqa(i+j)} + \text{c.c.}], \quad (4.1)$$

$$y_{i,j} = y_0(-1)^{i+j} + \sum_{0 < q < \pi/a} [y_q e^{iqa(i+j)} + \text{c.c.}]. \quad (4.2)$$

By this assumption the lattice degree of freedom is reduced from N^2 to $N - 1$; the uniform mode with $q = 0$ is excluded trivially. Then the original Hamiltonian can be written in the wave number representation as follows,

$$\begin{aligned} H = & \sum_{\mathbf{k},s} \varepsilon_{\mathbf{k}} c_{\mathbf{k},s}^\dagger c_{\mathbf{k},s} \\ & + \alpha \sum_{\mathbf{k},s} 2i(x_0 \sin k_x a + y_0 \sin k_y a) c_{\mathbf{k}+\mathbf{Q},s}^\dagger c_{\mathbf{k},s} \\ & + \alpha \sum_{0 < q < \pi/a} \sum_{\mathbf{k},s} 2 \left\{ e^{-iqa/2} \left[x_q \cos \left(k_x + \frac{q}{2} \right) a \right. \right. \\ & \left. \left. + y_q \cos \left(k_y + \frac{q}{2} \right) a \right] c_{\mathbf{k}+\mathbf{q},s}^\dagger c_{\mathbf{k},s} \right\} \end{aligned}$$

$$\begin{aligned}
& +e^{iqa/2} \left[x_q^* \cos \left(k_x - \frac{q}{2} \right) a \right. \\
& \left. + y_q^* \cos \left(k_y - \frac{q}{2} \right) a \right] c_{\mathbf{k}-\mathbf{q},s}^\dagger c_{\mathbf{k},s} \} \\
& + N^2 \frac{K}{2} (x_0^2 + y_0^2) \\
& + N^2 K \sum_{0 < q < \pi/a} (|x_q|^2 + |y_q|^2), \tag{4.3}
\end{aligned}$$

where the vector \mathbf{q} stands for (q, q) .

Thus, in order to obtain the electronic energy spectrum in the presence of the lattice distortions considered above, we have to solve the eigenvalue problem of the following form,

$$\begin{aligned}
\varepsilon \psi(k_x, k_y) = \varepsilon_{\mathbf{k}} \psi(k_x, k_y) & \\
& - 2i\alpha (x_0 \sin k_x a + y_0 \sin k_y a) \times \\
& \psi(k_x - Q_x, k_y - Q_y) \\
& + 2\alpha \sum_{0 < q < \pi/a} \left\{ e^{-iqa/2} \left[x_q \cos \left(k_x - \frac{q}{2} \right) a \right. \right. \\
& \left. \left. + y_q \cos \left(k_y - \frac{q}{2} \right) a \right] \psi(k_x - q, k_y - q) \right. \\
& \left. + e^{iqa/2} \left[x_q^* \cos \left(k_x + \frac{q}{2} \right) a \right. \right. \\
& \left. \left. + y_q^* \cos \left(k_y + \frac{q}{2} \right) a \right] \psi(k_x + q, k_y + q) \right\}, \tag{4.4}
\end{aligned}$$

where $\psi(k_x, k_y)$ means the wave function in the wave number representation. It should be noted that, in the above equation, only the combinations of k_x and k_y with a constant difference are involved. It is not difficult to understand from this fact that the Hamiltonian matrix whose original size is $N^2 \times N^2$ can be decomposed into N pieces each of which has a size $N \times N$. Therefore the most general eigenvalue problem eq. (3.1) is decoupled into N one dimensional problems in the present situation. Each eigenvalue equation of the form eq. (4.4) yields a set of N eigenvalues and N eigenfunctions. By solving N sets of eigenvalue problems for one set of $\{x_q, y_q\}$ and (x_0, y_0) , we end up with a set of N^2 eigenvalues and N^2 eigenfunctions. Sorting N^2 eigenvalues in increasing order, we determine the state index ν and attach it to each eigenvalue and eigenfunction as ε_ν and $\psi_\nu(k + k', k)$. If we note the periodicity of the wave functions in the \mathbf{k} -space, we have only to consider the range of k and k' such as $-\pi/a < k, k' \leq \pi/a$.

Next we have to discuss how to determine the set of variables, $\{x_q, y_q\}$ and (x_0, y_0) . They are determined so as to minimize the total energy of the system as done in § 3. The self-

consistent equations for these variables are written in the following form,

$$x_0 = -\frac{2i\alpha}{KN^2} \sum_{\nu}' \sum_{\mathbf{k}} \sin k_x a \psi_{\nu}^*(k_x + \pi/a, k_y + \pi/a) \times \psi_{\nu}(k_x, k_y), \quad (4.5)$$

$$y_0 = -\frac{2i\alpha}{KN^2} \sum_{\nu}' \sum_{\mathbf{k}} \sin k_y a \psi_{\nu}^*(k_x + \pi/a, k_y + \pi/a) \times \psi_{\nu}(k_x, k_y), \quad (4.6)$$

$$x_q = -\frac{2e^{iqa/2}\alpha}{KN^2} \sum_{\nu}' \sum_{\mathbf{k}} \cos\left(k_x - \frac{q}{2}\right) a \times \psi_{\nu}^*(k_x - q, k_y - q) \psi_{\nu}(k_x, k_y), \quad (4.7)$$

$$y_q = -\frac{2e^{iqa/2}\alpha}{KN^2} \sum_{\nu}' \sum_{\mathbf{k}} \cos\left(k_y - \frac{q}{2}\right) a \times \psi_{\nu}^*(k_x - q, k_y - q) \psi_{\nu}(k_x, k_y), \quad (4.8)$$

where the sum over ν is restricted to the occupied states. We have omitted complex conjugate forms of eqs. (4.7) and (4.8). It should be noted that for each ν the corresponding wave function is finite only when $k_x - k_y = \text{const.}$, though this constant depends on ν .

In the present calculation scheme, we have only to diagonalize N different $N \times N$ matrices instead of a single $N^2 \times N^2$. This makes the computational load much lighter, and therefore we can treat far larger system than in the case where we deal with two dimensional problems directly.

In Figs. 4 and 5 we show the wave number dependences of the amplitudes and the phases of x_q 's and y_q 's which have been obtained by solving the self-consistent equations for the system size $N = 128$ (the total number of lattice points = 128×128) and the coupling constant $\alpha = 4.0 \text{ eV/\AA}$ ($\lambda = 0.30$). The initial condition used in this iterative calculation is $\text{Re } x_q = \text{Im } x_q = x_{\text{in}}$ (some constant of the order of $10^{-2}a$) for $q = 2\pi/Na$, $x_q = 0$ for other q and $y_q = 0$ for all q , where q is restricted in the region $0 < q < \pi/a$, and $x_0 = y_0 = x_{\text{in}}$. The final results does not depend on the values of x_{in} . The results for different types of initial conditions will be discussed later.

The amplitudes of x_q and y_q are completely equal to each other and are found to vanish at q values which are even integer times $2\pi/Na$, though, as a matter of course, $q = \pi/a$ is exceptional. As for the phases, we find the relation $\arg(x_{q_1}) + \arg(x_{q_2}) = \arg(y_{q_1}) + \arg(y_{q_2}) = 0 \pmod{\pi}$ for q_1 and q_2 satisfying $q_1 + q_2 = \pi/a$. This will be reasonable if we remind us the second order perturbation mechanism of the Peierls gap formation.

Once we know the values of $\{x_q\}$, $\{y_q\}$, x_0 and y_0 , we can obtain N eigenenergies for each set of N electronic wave vectors. Assuming that the energy of the lower (higher) band is an increasing (decreasing) function of the distance from the line $k_x + k_y = 0$, we can assign the

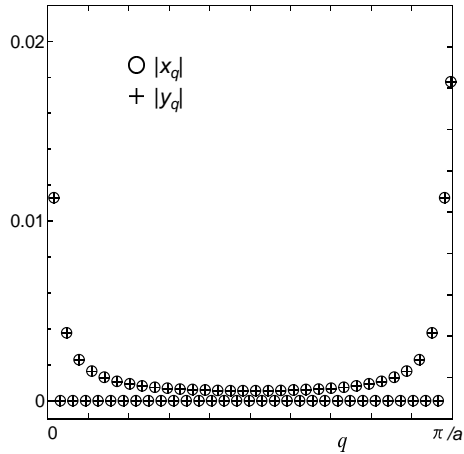


Fig. 4. The q dependences of the amplitudes $|x_q|$ and $|y_q|$. The values of $|x_0|$ and $|y_0|$ are also plotted. The system size is $N = 128$, and the coupling constant is $\alpha = 4.0\text{eV}/\text{\AA}$ ($\lambda = 0.30$).

energy versus \mathbf{k} relation. The dispersion relation obtained in this way is shown in Fig. 6 for the case with $\alpha = 6.0\text{eV}/\text{\AA}$ ($\lambda = 0.69$).¹⁰⁾ Only the lower band which is fully occupied in the ground state is shown along the lines depicted in the sub-figure. Because of the electron-hole symmetry of the system the dispersions of the unoccupied levels are the same as those shown in Fig. 6 except for the sign of energy.

Thus by assigning the dispersion relation for all the points in the \mathbf{k} -space, we can now see the gap structure on the Fermi surface. As will be clear from Fig. 6, the gap is constant along the line $(-\pi/a, 0) - (0, \pi/a)$. On the other hand the gap structure along the line $(0, \pi/a) - (\pi/a, 0)$ is not so simple as will be found from Fig. 7, where the dispersion curves of upper and lower bands along the line $(0, \pi/a) - (\pi/a, 0)$ are shown for the cases with a couple of different values of the electron-lattice coupling constant.

In contrast to the asymmetrically dimerized case (Fig 1), the gap does not vanish at any point, taking almost the same value as that at $(\pi/2a, \pi/2a)$. It will be noteworthy that the gap is not minimum at $\mathbf{k} = (0, \pi/a)$ or $(\pi/a, 0)$ and that the multi-mode effect is almost negligible around the point $\mathbf{k} = (\pi/2a, \pi/2a)$. The position of the gap minimum depends on the coupling constant. In the same figure, the dispersions in the asymmetrically dimerized case for each coupling constant are shown for comparison.

In order to see the size dependence of the gap Δ , we plot in Fig. 8 the gap at three different

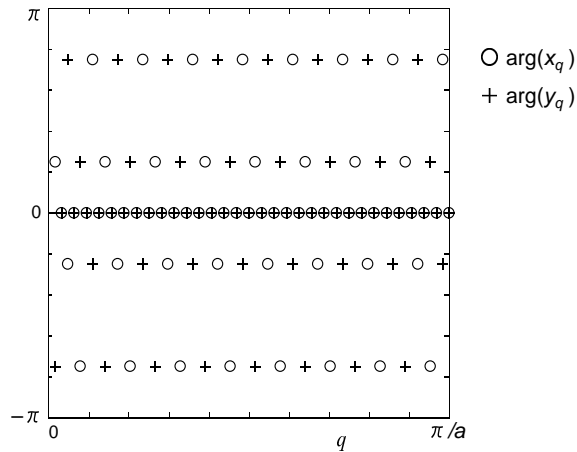


Fig. 5. The q dependences of the phases $\arg(x_q)$ and $\arg(y_q)$. The values of $\arg(x_0)$ and $\arg(y_0)$, which are zero in this example, are also given for comparison. The system size is $N = 128$, and the coupling constant is $\alpha = 4.0\text{eV}/\text{\AA}$ ($\lambda = 0.30$).

points on the line $(0, \pi/a) - (\pi/a, 0)$, as indicated in the inset, for a coupling constant $\lambda = 0.69$ ($\alpha = 6.0\text{eV}/\text{\AA}$). From this figure we find that $N = 128$ belongs to the large size limit as far as the behavior of the gap concerns and that in the large size limit the gaps Δ_1 and Δ_2 at $(\pi/2a, \pi/2a)$ and $(0, \pi/a)$ are indistinguishable though the value of Δ_3 remains smaller than Δ_1 and Δ_2 . For smaller values of the coupling constant, a similar tendency is found, but the large size limit is seen only at larger system sizes, although $N = 128$ is sufficiently large even for $\alpha = 4.0\text{eV}/\text{\AA}$.

As indicated by the results shown above, the lowest energy state obtained here is not completely symmetric with respect to x and y directions. This fact means that there exist at least two degenerate states where the roles of x and y are interchanged.

In order to check other degeneracy of the lowest energy states, we have studied what kind of distortion patterns could be obtained when we change the initial distortions in the iterative calculation. As a result, we got many different distortion patterns with the same energy as that of the distortion pattern shown in Figs. 4 and 5. Some are different only in the phases of the Fourier components of the distortion. Some show completely different behaviors. Among them there is a pattern where the nonvanishing Fourier components are $x_{\pi/2a}$, $y_{\pi/2a}$, x_0 and y_0 and other components are zero. In these degenerate states, not only the total energy but

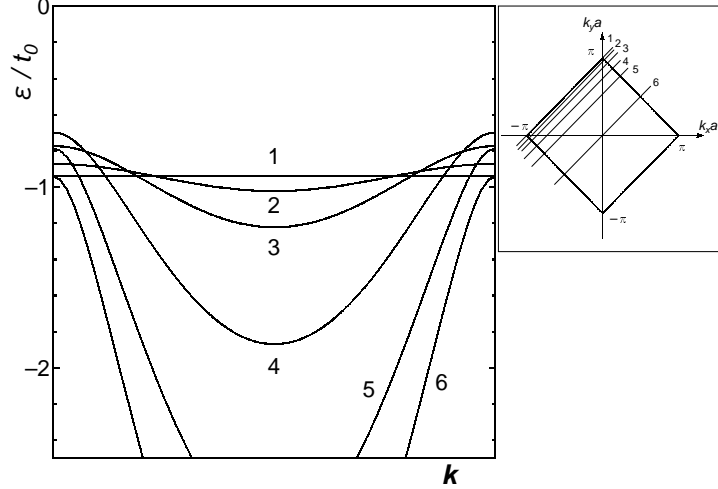


Fig. 6. The dispersion relations of occupied levels for $\alpha = 6.0\text{eV}/\text{\AA}$ ($\lambda = 0.69$) and the system size 128×128 . The wave numbers are changed along the lines indicated in the sub-figure.

also the electronic part and the lattice potential part are also the same, respectively. At the moment we cannot say how many states are degenerate. Detailed analysis of the degeneracy problem is left for a future work.

§5. Summary and Discussion

The lowest energy state of a two dimensional electron-lattice system with a half-filled electronic band and with a square lattice structure is studied within the SSH-type model extended to two dimensions. On the contrary to the previous common understanding that only the lattice distortion with the nesting vector $\mathbf{Q} = (\pi/a, \pi/a)$ is frozen in the lowest energy state,³⁾ many modes are found to be frozen in the real lowest energy state. The state discussed by Tang and Hirsch³⁾ might be a local minimum but it is not the absolute minimum of energy. This is because the Peierls gap vanishes at $(\pi/a, 0)$ and $(0, \pi/a)$ due to the wave number dependence of the electron-lattice coupling term. We have pointed out that the second order perturbation mechanism of the Peierls gap formation is important. Numerical minimization of the total energy leads to the conclusion that many modes having the wave number parallel to \mathbf{Q} contribute to the formation of the gap. Assuming this is the case, we can reduce the two-dimensional problem into one-dimensional problems by using the wave number representation of the Hamiltonian as discussed in § 4. In this formulation it is

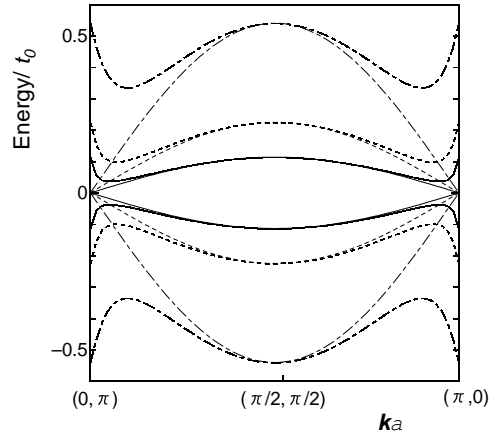


Fig. 7. The dispersions of the highest occupied and lowest unoccupied levels along the line $(0, \pi/a) - (\pi/a, 0)$. Three different values of electron-lattice constant are considered, $\alpha[\text{eV}/\text{\AA}] = 4.0$ ($\lambda = 0.30$); continuous thick line, 4.4 (0.37); dotted line and 5.2 (0.52); dash-dotted line. The similar dispersions for the asymmetric dimerized state (Fig. 1) are also shown by the same type thinner lines.

possible to treat far larger system sizes than in the case where we search a minimum energy state of the two-dimensional system directly. The electronic energy dispersion and the gap structure on the Fermi surface have been analyzed. Although the wave number dependences of the amplitudes and phases of condensed modes look to show a certain symmetry in the x and y directions, the electronic structures are not necessarily symmetric.

What we have shown in this paper is not the unique lowest energy state. A preliminary study indicates there might be infinite number of degenerate ground states. The degree of degeneracy is not known at the moment. It is not clear also what kind of symmetry is relevant to this degeneracy. Detailed study of the degeneracy problem is left for the future work. Nevertheless it will be worthwhile to mention that this type of degeneracy of the ground state yields the possibility of the formation of domain walls like the solitons in the one-dimensional systems where the number of degenerate ground state is only two.^{6, 11, 12} This kind of domain walls connecting two different ground states may supply interesting properties of the two-dimensional electron-lattice systems just as the charged and neutral solitons in polyacetylene did.

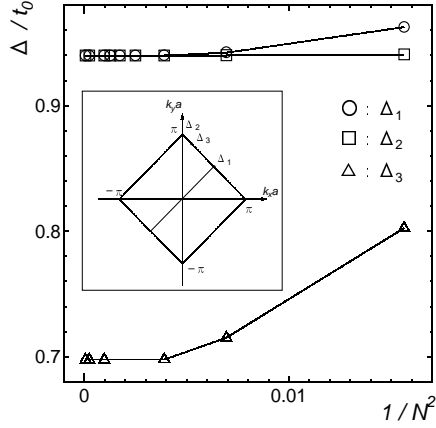


Fig. 8. The system size dependence of the gap Δ in the electronic spectrum at different points on the line $(0, \pi/a) - (\pi/a, 0)$. The coupling constant is fixed at $\lambda = 0.69$.

Acknowledgments

The authors are grateful to Professor Y. Wada for useful comment on existing references.

-
- [1] R.E. Peierls: *Quantum theory of Solids* (Clarendon Press, Oxford, 1955).
 - [2] K. Machida and M. Kato: Phys. Rev. **B36** (1987) 854.
 - [3] S. Tang and J.E. Hirsch: Phys. Rev. **B37** (1988) 9546.
 - [4] R.T. Scalettar, N.E. Bickers, and D.J. Scalapino: Phys. Rev. **B37** (1989) ???
 - [5] S. Mazumdar: Phys. Rev. **B39** (1989) 12324.
 - [6] W. P. Su, J. R. Schrieffer, and A. J. Heeger: Phys. Rev. Lett. **42** (1979) 171, Phys. Rev. **B22** (1980) 2099.
 - [7] S. Stafström and K.A. Chao: Phys. Rev. **B29** (1984) 7010; *ibid* **30** (1984) 2098.
 - [8] A. Terai and Y. Ono: J. Phys. Soc. Jpn. **55** (1986) 213.
 - [9] Because of square lattice symmetry, the wave vectors for which the Fourier components are finite can be $(q_d, -q_d)$ or $(-q_d, q_d)$. We do not distinguish these cases from the case with (q_d, q_d) .
 - [10] We have taken a larger coupling constant for showing the dispersion, since the detailed structures can be seen more clearly than those for smaller values of the coupling constant.
 - [11] M.J. Rice: Phys. Lett. **71A** (1979) 152.
 - [12] H. Takayama, Y.R. Lin-Liu, and K. Maki: Phys. Rev. **B21** (1980) 2388.